

# Acute Stress Increases Striatal Connectivity With Cortical Regions Enriched for $\mu$ and $\kappa$ Opioid Receptors

Peter Zhukovsky, Maria Ironside, Jessica M. Duda, Amelia D. Moser, Kaylee E. Null, Maeva Dhaynaut, Marc Normandin, Nicolas J. Guehl, Georges El Fakhri, Madeline Alexander, Laura M. Holsen, Madhusmita Misra, Rajesh Narendran, Jocelyn M. Hoye, Evan D. Morris, Shiba M. Esfand, Jill M. Goldstein, and Diego A. Pizzagalli

## ABSTRACT

**BACKGROUND:** Understanding the neurobiological effects of stress is critical for addressing the etiology of major depressive disorder (MDD). Using a dimensional approach involving individuals with differing degree of MDD risk, we investigated 1) the effects of acute stress on cortico-cortical and subcortical-cortical functional connectivity (FC) and 2) how such effects are related to gene expression and receptor maps.

**METHODS:** Across 115 participants (37 control, 39 remitted MDD, 39 current MDD), we evaluated the effects of stress on FC during the Montreal Imaging Stress Task. Using partial least squares regression, we investigated genes whose expression in the Allen Human Brain Atlas was associated with anatomical patterns of stress-related FC change. Finally, we correlated stress-related FC change maps with opioid and GABA<sub>A</sub> (gamma-aminobutyric acid A) receptor distribution maps derived from positron emission tomography.

**RESULTS:** Results revealed robust effects of stress on global cortical connectivity, with increased global FC in frontoparietal and attentional networks and decreased global FC in the medial default mode network. Moreover, robust increases emerged in FC of the caudate, putamen, and amygdala with regions from the ventral attention/salience network, frontoparietal network, and motor networks. Such regions showed preferential expression of genes involved in cell-to-cell signaling (*OPRM1*, *OPRK1*, *SST*, *GABRA3*, *GABRA5*), similar to previous genetic MDD studies.

**CONCLUSIONS:** Acute stress altered global cortical connectivity and increased striatal connectivity with cortical regions that express genes that have previously been associated with imaging abnormalities in MDD and are rich in  $\mu$  and  $\kappa$  opioid receptors. These findings point to overlapping circuitry underlying stress response, reward, and MDD.

<https://doi.org/10.1016/j.biopsych.2024.02.005>

Acute stress has substantial effects on brain function (1) and cognitive processes (2) that help humans adapt and flexibly respond to the environment (3). However, when stress is chronic, severe, or perceived as uncontrollable, it can detrimentally impact health, especially in individuals with increased vulnerability to major depressive disorder (MDD) (4–6). Consistent with this, dysfunctional stress systems have been implicated in a number of disorders, most notably MDD. Specifically, stressful life events are likely to trigger a major depressive episode for many individuals (7). These effects of severe stressors may stem from interactions between the stress and reward-processing systems (5).

The neurochemical changes that facilitate an organism's response to stress work in different spatial and temporal domains (3). Acute stress is typically associated with increased autonomic and central nervous system arousal that allows for high behavioral flexibility, adaptive allocation of cognitive resources, and attention switching (2,8,9). Increased vigilance and alertness that allow an organism to immediately assess

and respond to a stressor are typically subserved by the rapid activation of the monoamine system, including the release of noradrenaline from the locus coeruleus (10) and serotonin from the dorsal raphe as well as recruitment of the prefrontal cortex (3). For example, neuroimaging studies have shown increased connectivity and activation of the salience/ventral attention network during acute stress (1). These changes are accompanied and modulated by increased levels of corticotropin-releasing factor (3). Conversely, the effects of corticosteroids occur on a slower timescale (11) and preferentially target the hippocampus (3,12). Plasma corticosterone levels peak about 20 to 30 minutes following the stressor, and brain levels of corticosterone peak minutes later (12,13) and can suppress noradrenergic activity, leading to stress relief (3). During the stress termination phase, endogenous opioids such as enkephalin are thought to activate  $\mu$  opioid receptors (14), which leads to a shift toward lower tonic and increased phasic locus coeruleus activity (8). Activation of the  $\mu$  opioid receptors in the amygdala has also been linked to coping with stress (15).

Moreover, stress increases amygdala activation and connectivity to the striatum (16), potentiating stimulus-response learning (17). In a well-functioning stress system, the hippocampus regulates the release of corticosteroids (18,19), which can trigger the release of endorphins (20), thus leading to termination of the stress response.

Convergent evidence from animal and human studies implicates the opioid system in stress response. For example, the endogenous opioid system exerts analgesic effects under stressful conditions (21–23). In monkeys, a single nucleotide polymorphism in the  $\mu$  opioid receptor influenced individual variability in stress response (24). The opioid system has also been implicated in MDD because women with MDD showed lower  $\mu$  opioid receptor availability than healthy women (25), with lower  $\mu$  opioid receptor availability being linked to negative mood. In addition, animal models have shown that stress-induced release of corticotropin-releasing hormone leads to  $\kappa$  opioid activation and downstream extracellular serotonin availability, linked to dysregulated emotion and motivation (26,27). Therefore,  $\kappa$  opioid signaling is a novel target in the treatment of depression (28–30) and in stress-related disorders more generally. In addition, preclinical studies have described upregulation of nociceptin (NOP) receptor signaling in stress responses, and NOP blockage has antidepressant-like effects (31,32).

However, more evidence is needed to understand the neurobiological effects of stress on functional connectivity (FC) in individuals with varying MDD vulnerability (e.g., healthy control participants, individuals with remitted depression, individuals with current depression). Neuroimaging modalities do not provide information about molecular properties of brain tissue, but transcriptomic similarity analyses (33,34) can provide insight into the molecular correlates of stress responses/regulation (35–37). Previous studies of imaging transcriptomics have consistently implicated somatostatin-expressing cells in MDD (34,38). Notably, a large-scale analysis of the ENIGMA (Enhancing Neuro Imaging Genetics through Meta Analysis) data has shown cortical thinning in MDD in areas with higher proportions of microglia and astrocytes (39). As a result, MDD has been hypothesized to be driven in part by interneuron and glial dysfunction and by dysregulated apoptosis and neuroinflammation processes more generally (39–41). Imaging transcriptomics has not yet been applied in the context of acute, provoked stress, and it may help improve our understanding of the transcriptomic signal common to MDD and stress circuitry. It is a promising method (36,41,42) that identifies genes with anatomical expression maps that are similar to the brain maps of the effects measured using noninvasive magnetic resonance imaging (MRI).

We hypothesized that a potent psychosocial stressor that included the Montreal Imaging Stress Task (MIST) paradigm (43) would increase the connectivity of salience and frontoparietal networks to cortical and subcortical regions in healthy participants and those with current and remitted MDD. In addition, given the role of the opioid system in stress and reward processing, we expected stress to strengthen FC between subcortical regions rich in opioid receptors (e.g., nucleus accumbens) and between the amygdala and cortical regions that show high levels of  $\mu$  and  $\kappa$  opioid and NOP receptors. Taken together, the findings uncover imaging correlates of stress, highlighting the role of the opioid system

alongside other molecular markers such as somatostatin neurons.

## METHODS AND MATERIALS

### Participants

One hundred thirty unmedicated participants (ages 18–25 years), stratified by sex, were recruited from the community. Among these, 129 participants completed multimodal imaging (functional MRI [fMRI]) while undergoing negative stress paradigms. Our sample included 44 healthy control participants, 42 euthymic individuals with remitted MDD, and 43 individuals with current MDD (all participants were unmedicated). Female participants were scanned during the follicular phase of their menstrual cycle. Participants were excluded if their MRI data did not pass quality control, which resulted in 125 participants with at least one run of usable fMRI data (see the [Supplement](#)). After quality checks of excessive motion during baseline or stress conditions, the final sample included 115 participants (37 control, 39 active MDD, and 39 remitted MDD). Participants provided written informed consent, and ethical approval was obtained from the Massachusetts General Brigham Institutional Review Board. Participants completed the Structured Clinical Interview for DSM-5, which was administered by a masters- or Ph.D.-level clinical interviewer. Exclusion criteria included other comorbid psychiatric disorders (except for mild cannabis use disorders in active or remitted MDD, simple phobia, social anxiety, and generalized anxiety disorder if secondary to MDD), use of psychoactive drugs, past moderate-severe substance use disorder, and more than 5 alcohol-related blackouts (see the [Supplement](#) for full details, including how remitted MDD was defined). An overview of the study procedures is shown in [Figure S1](#) in [Supplement 1](#).

### Data Processing

**MRI Acquisition.** High-resolution functional and structural MRI data were acquired on a 3T Siemens MAGNETOM Prisma scanner (Siemens Medical Systems) with a 64-channel head coil (44) ([Supplement](#)).

**fMRI Processing.** Functional and structural MRI data were preprocessed using fMRIPrep. Following preprocessing, we regressed out 24 motion parameters (45): 6 motion parameters, average signal from the white matter and cerebrospinal fluid and their first- and second-order temporal derivatives, and applied a 6-mm smoothing kernel. fMRIPrep outputs were registered from the Nlin6 (MNI152) space to the FreeSurfer *fsaverage* space (*mri\_vol2surf*). We used the HCP (Human Connectome Project) cortical parcellation in *fsaverage* surface space, averaging across pairs of 180 bilateral regions (46), and the Harvard-Oxford Atlas subcortical parcellation in MNI152 volumetric space to extract time series. We obtained global cortical FC measures for all cortical regions by calculating a  $180 \times 180$  connectivity matrix between each pair of bilateral regions in the HCP parcellation, excluding the values along the diagonal, and averaging each of the 180 rows. We also constructed subcortical-to-cortical connectivity maps for the left and right nucleus accumbens, caudate, putamen, amygdala, and hippocampus.

**Allen Human Brain Atlas.** Microarray data from the Allen Human Brain Atlas (AHBA) were preprocessed and mapped to the HCP parcellation using the *abagen* toolbox with default settings (42). As part of the process, postmortem probes were mapped onto the HCP parcellation (46), with 171 of 180 regions mapping onto a microarray probe (Tables S1–S13 in Supplement 2). We analyzed MRI statistics from only the left hemisphere because 4 of the 6 AHBA donors only had samples taken from their left hemisphere.

**Positron Emission Tomography Receptor Maps.** Average receptor distribution maps for [<sup>11</sup>C]carfentanil and [<sup>11</sup>C]flumazenil in MNI152 space were obtained from Hansen *et al.* (47), who obtained them from (48–50). Specifically, [<sup>11</sup>C]carfentanil was used to map  $\mu$  opioid receptors (48,49), and [<sup>11</sup>C]flumazenil was used to map GABA<sub>A</sub> (gamma-aminobutyric acid A) receptors (50). In addition, a  $\kappa$  opioid receptor map was obtained from 28 healthy participants who were studied by Vijay *et al.* (51). The NOP receptor map was obtained from data acquired from 68 healthy participants studied by Narendran *et al.* (52) that were reanalyzed by our team using voxelwise Logan graphical analysis. The mean receptor maps in MNI152 space are available upon request. All group average positron emission tomography (PET) maps were derived from healthy participants.

**Cortisol.** More details on blood sampling and cortisol processing can be found in the Supplement [also see (9,44)]. Following previous studies (53), we calculated the increase in cortisol between baseline and the time point after the hard MIST stress condition using the area under the curve with respect to ground method (53). Prior to the hard MIST condition, participants completed the Maastricht Acute Stress Test (MAST) (54).

### Statistical Analysis

First, we used mixed-effects linear models in MATLAB version R2022a (The MathWorks, Inc.) (*fitlme*) to assess the effects of stress, operationalized as the hard MIST condition compared with baseline, on global cortical connectivity and subcortical-to-cortical connectivity while covarying for clinical group status, sex, age, and mean framewise displacement (FD) (model 1). To assess the within-participant effects of stress, participant-level random intercepts were included. We also tested for group  $\times$  stress interactions, contrasting participants with MDD with healthy control participants and participants with remitted MDD with healthy control participants separately (Supplement).

$$\text{Model 1: } FC \sim \text{mean FD} + \text{sex} + \text{age} + \text{group} + \text{stress} + (1 | \text{Participant}) \quad (1)$$

Within each of the 11 sets of 180 tests for global cortical, left and right accumbens, caudate, putamen, amygdala, and hippocampus FC, we controlled for multiple comparisons using false discovery rate (FDR) [Benjamini-Hochberg FDR (55)]  $q < .05$ . The distribution of stress effects was plotted using the Yeo 7 network parcellation (56).

Next, we tested spatial associations between the brain maps reflecting the effects of stress on FC from the above linear models with 1) postmortem gene expression maps obtained from the AHBA and 2) anatomical maps of PET receptor binding in the brain. We used partial least squares (PLS) regression (33,57,58) to identify genes that showed an anatomical expression map similar to the stress effect map. The  $171 \times 15,631$  predictor matrix in the PLS model had 171 rows for each of the HCP regions and 15631 genes that passed quality control. We ran a total of 11 PLS models. In each model, the outcome matrix was a  $171 \times 1$  vector of  $t$  statistics reflecting the effects of stress on global FC and on FC of the left and right accumbens, caudate, putamen, hippocampus, and amygdala with 171 cortical regions. We tested the significance of the overall model using permutation testing ( $n = 5000$  permutations) (33,57). For each gene, we calculated a bootstrapped weight reflecting the robustness of that gene's contribution to the model by dividing each gene's weight in the original PLS by the standard deviation of that gene's weights in the bootstrapped PLSs ( $n = 5000$ ) (33). Since 11 PLS models were fitted, the overall model significance was set at  $p < .0045$  (.05/11 PLS models).

We also tested for spatial associations between anatomical maps of PET receptor binding and stress effects on FC. To assess significance after multiple comparison correction, we set the  $p$  value at  $p < .0013$  (.05 /10 regions/4 tracers).

Hypergeometric tests with area under the receiver operating curve analyses were used to test for enrichment of MDD-related genes in a list of genes ranked by weights that emerged from the PLS models (59). This analysis allowed us to evaluate whether gene weights that emerged from the PLS models were higher for genes that had been identified in previous studies of MDD, including genome-wide association studies (60) and transcriptomic similarity methods (34). In addition, we performed the hypergeometric tests on the triplet of somatostatin markers [*SST*, *CORT*, *NPY* (34)]. Finally, we used the *clusterProfiler* package in R (version 4.2.1) to test whether significant genes identified by our PLS models ( $|Z| > 4$ ) were associated with specific gene ontology terms.

## RESULTS

### Main Effects of Stress on Global Cortical and Subcortical FC

Global cortical connectivity was highest in sensorimotor areas such as the visual cortex (Figure 1A). Critically, acute stress increased global cortical connectivity of frontoparietal and dorsal attentional areas and decreased global connectivity of anterior and posterior medial default mode areas across all participants (Figure 1C, E). Moreover, acute stress increased connectivity of the striatum and the amygdala with ventral attention and frontoparietal areas (Figure 1B, D, F). In particular, stress increased the connectivity of the accumbens, caudate, putamen, and amygdala with the insular cortex. No significant main effects of stress on left hippocampal, left amygdala, and right accumbens connectivity to the cortex were found after multiple comparison correction (FDR-corrected  $p > .05$ ).

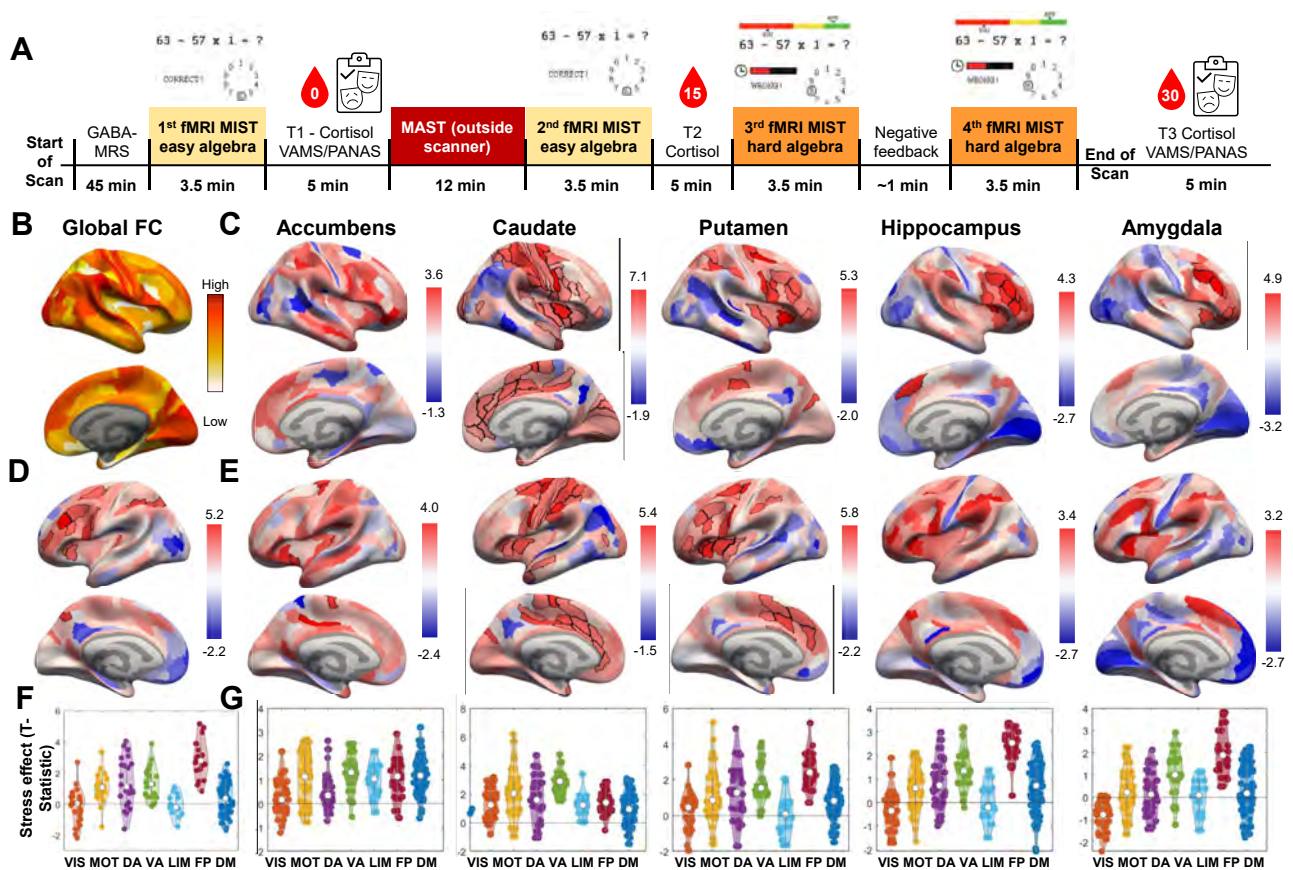


**Figure 1.** An overview of the study design adapted from Ironside *et al.* (44) is shown in (A). Effects of stress on global cortical connectivity (D) and on subcortical-to-cortical connectivity of the left (C) and right (E) accumbens, caudate, putamen, hippocampus, and amygdala. Mean global FC across all participants is shown in (B). Regional effects of stress on cortical and subcortical connectivity grouped by Yeo 7 network are plotted in (F) and (G). Bilateral cortical regions [ $n = 180$  (46)] were used. We showcase the  $t$  statistics to visualize the effects of stress. Significant regions are highlighted with a black outline. Yeo 7 networks included the VIS, MOT, DA, VA, LIM, FP, and DM networks. Main analyses compared the first and the fourth runs of fMRI, i.e., the easy and hard MIST conditions. More details about the study design can be found in the Supplement. DA, dorsal attention; DM, default mode; FC, functional connectivity; fMRI, functional magnetic resonance imaging; FP, frontoparietal; GABA, gamma-aminobutyric acid; LIM, limbic; MAST, Maastricht Acute Stress Test; MIST, Montreal Imaging Stress Task; MOT, motor; MRS, magnetic resonance spectroscopy; PANAS, Positive and Negative Affect Schedule; T, time; VA, ventral attention; VAMS, Visual Analogue Mood Scale; VIS, visual.

### Change in Cortisol Levels and FC Following the MAST and MIST

Using partial correlations (covarying for age, sex, and group), we found that the increase in cumulative cortisol levels (area under the curve with respect to ground) from baseline over the period of acute stress was positively associated with baseline FC of the putamen with insular, dorsolateral prefrontal, and motor regions (Figure S6 in Supplement 1) (FDR-corrected  $p < .05$ ). However, no significant associations were found between change in FC and change in cortisol levels. In supplementary analyses, we aimed to better understand the temporal profile of changes in cortisol and FC after the MAST and then during the hard MIST compared with baseline. We found the greatest cortisol increases following the MAST, with only small increases following the MIST. Conversely, we found very few significant changes in FC following the MAST, with the greatest FC changes during the hard MIST.

### Stress Effects on Subcortical FC Reflect Spatial Patterns of $\mu$ and $\kappa$ Opioid and GABA Gene Expression

In 11 PLS regression models, we evaluated whether the cortical maps of stress effects on global connectivity and connectivity of the left and right accumbens, caudate, putamen, hippocampus, and amygdala were spatially associated with gene expression maps from the AHBA. We found that several PLS models explained significantly more variance (between 20% and 25%,  $p < .0045$ ) (Figure 2A, B, F; Tables S1–S13 in Supplement 2) in the cortical maps of stress effects than that expected by chance. Significant multivariate associations were found for the stress effects on global FC, left and right putamen, left caudate and hippocampus, and right amygdala. Among genes with anatomical expression patterns similar to the effects of stress on subcortical connectivity, notable genes were  $\mu$  and  $\kappa$  opioid receptor genes (Figure 2C,

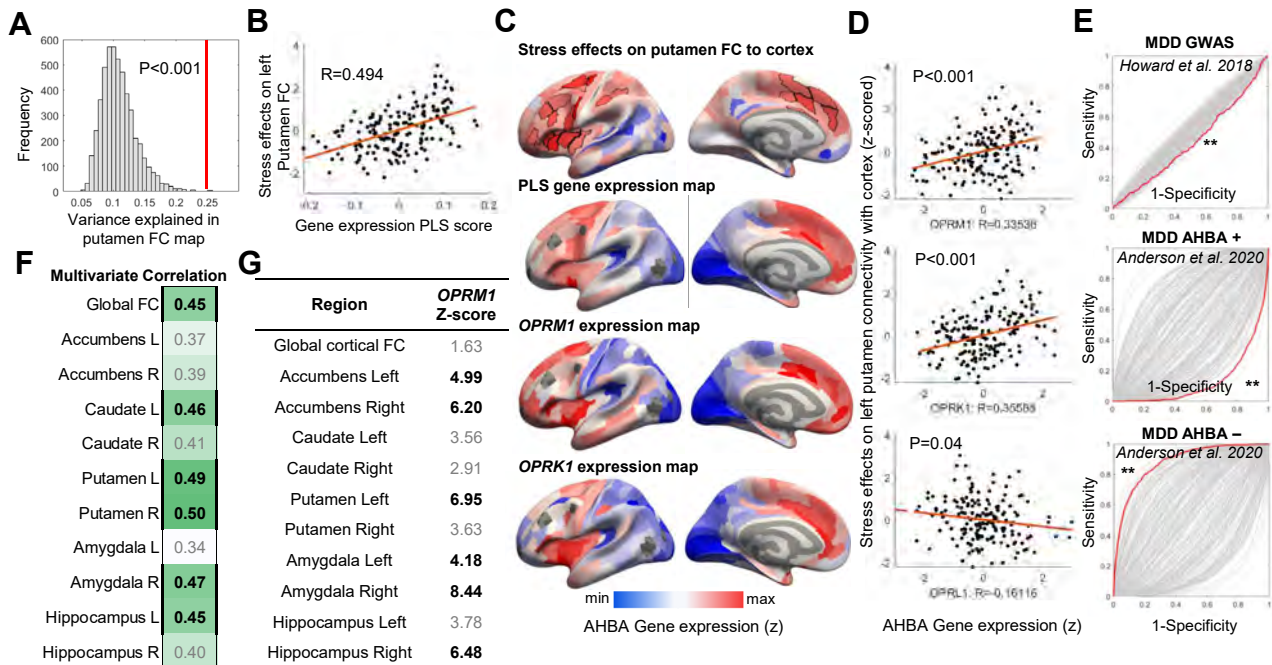


**Figure 2.** The PLS model showed that gene expression maps shared a significant portion of variance with the anatomical map of stress effects on putamen FC (A, B). Significant multivariate associations between gene expression and anatomical maps of stress effects on left caudate, hippocampus, right amygdala, and global cortical FC were found (F) (Tables S1–S13 in Supplement 2). We present multivariate correlations for the putamen in (B) and for all brain maps in (F). Significant PLS models ( $p < .0045$ ) are highlighted in bold. Several genes were correlated with accumbens FC, including  $\mu$  and  $\kappa$  opioid receptor genes (C, D). Mean expression maps of *OPRM1* and *OPRK1* are shown in (C) alongside the overall PLS1 gene expression map. *OPRM1* expression was also significantly associated with stress effects on the connectivity of other subcortical regions (G). Our analyses identified genes previously implicated in GWAS and transcriptomic studies of MDD (E). \*permutation  $p < .05$ . AHBA, Allen Human Brain Atlas; FC, functional connectivity; GWAS, genome-wide association study; L, left; MDD, major depressive disorder; PLS, partial least squares; R, right.

D), as well as somatostatin marker genes (Tables S1–S13 in Supplement 2; Figure S7 in Supplement 1).

Genes identified in our PLS analyses of stress effects on putamen connectivity in particular have emerged in genome-wide association studies of MDD (61) as well as MDD transcriptomic similarity analyses (34) (Figure 2E). Similarly, somatostatin marker genes showed higher-than-chance scores in the PLS that tested the transcriptomic correlates of stress effects on putamen connectivity (Figure S7 in Supplement 1). Many of our PLS models showed high positive association scores for genes such as *SST*, *OPRM1*, and *OPRK1* (Tables S1–S13 in Supplement 2; Figure 2G) that are preferentially expressed in insular and medial prefrontal regions. Gene ontology analyses of significant genes ( $|Z| > 4$ ) from all PLS models implicated terms related to metabolic processes and cell-to-cell signaling (Figure S8 in Supplement 1).

### Stress Effects on Subcortical FC Reflect Spatial Patterns of PET Distribution of $\kappa$ and $\mu$ Opioid Receptors

We found a significant correlation between the spatial maps of the effects of stress on FC of the putamen and amygdala across participants and the spatial maps of average  $\mu$  and  $\kappa$  opioid receptor distribution obtained from separate, healthy samples (Figure 3A–D). Stress also increased the FC of the nucleus accumbens with areas that are rich in  $\mu$  opioid receptors (Figure 3C). We found mostly negative, but weak,

associations between stress effects on subcortical-to-cortical FC and NOP1A receptor distribution (Figure 3E). Interestingly, stress increased the connectivity of the caudate and putamen with regions that have a relatively lower density of GABA<sub>A</sub> receptors (Figure 3F, G). No significant associations with GABA<sub>A</sub> or NOP maps were found for stress effects on the connectivity of the accumbens, amygdala, or hippocampus.

### DISCUSSION

Consistent with recent meta-analytic evidence (30), we demonstrated in a sample of participants differing in MDD risk that acute stress increased global cortical connectivity in the frontoparietal and dorsal attention regions and increased subcortical connectivity to frontoparietal salience and motor network regions. Critically, stress increased the connectivity of the putamen and the amygdala with medial and lateral prefrontal regions that preferentially express opioid receptor genes and somatostatin gene markers in a postmortem sample (AHBA), showing a pattern similar to that found in neuroimaging transcriptomics studies of MDD (34,38) and genome-wide association studies of MDD (60). Stress-induced increases in subcortical connectivity were most prominent in  $\mu$  and  $\kappa$  opioid receptor-rich areas, as quantified by PET-derived receptor density maps obtained from previous studies (51,52,62). Conversely, GABA<sub>A</sub> receptors were more widely distributed across the brain and were not concentrated in

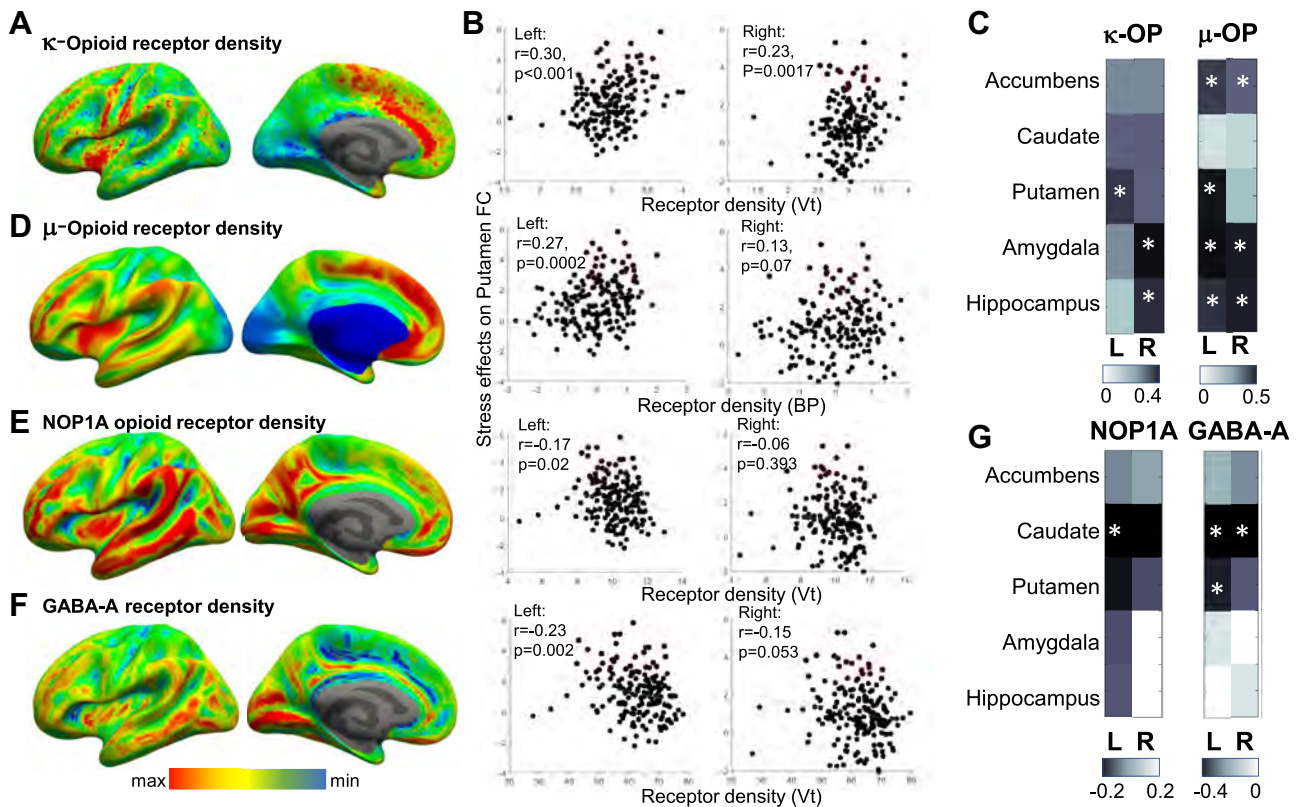


**Figure 3.** Correlation analyses showed several significant associations between anatomical patterns of stress effects on subcortical connectivity and brain maps of  $\kappa$  opioid (A),  $\mu$  opioid (D), nociceptin (E), and GABA<sub>A</sub> (F) receptor distribution in healthy participants. In particular, stress increased connectivity of the putamen and amygdala with both  $\kappa$  and  $\mu$  opioid-rich areas (C). However, GABA<sub>A</sub> and nociceptin receptor densities were not concentrated in the insular and medial prefrontal areas, resulting in nonsignificant or negative correlations between stress effect maps and the respective receptor maps (G). Scatterplots of these associations are shown in (B). \* $p < .001$ . BP, binding potential; FC, functional connectivity; GABA, gamma-aminobutyric acid; L, left; R, right; Vt, distribution volume.

insular and medial prefrontal areas whose connectivity with the striatum and amygdala was increased under stress. NOP1A receptors were not specific to insular and medial prefrontal areas because they were also found in lateral temporal areas, the visual cortex, and the precuneus.

In this novel imaging transcriptomics study of stress effects on FC, we showed that stress increased FC in opioid receptor-rich circuits (including the nucleus accumbens, putamen, amygdala, and the insular, inferior frontal, and medial prefrontal areas), providing further evidence for the role of the opioid system in acute negative stress response. The endogenous opioid system, especially the  $\mu$  and  $\kappa$  subtypes, has been linked to dysregulated mood, processing of negative social interactions, and social anhedonia in MDD (30,63). In particular, considerable efforts are being directed toward developing safe and effective agents that target the endogenous opioid system in depression (28–30,63).

In addition to the role of  $\mu$  and  $\kappa$  opioid receptor genes, we identified a number of other genes transcriptionally linked to the neurobiological effects of stress including the somatostatin markers and GABRA3 and GABRA5 receptor genes. Comparison of the genes identified in our analyses with previous imaging transcriptomics studies of MDD (34,38) revealed

strong overlap in the genes identified, which suggests that MDD dysfunction occurs in neural circuits that also mediate the acute stress response. Stress increased accumbens connectivity with insular and medial prefrontal areas, which also show cortical thinning in MDD (34,57). In particular, Anderson *et al.* (34) found high negative association scores for genes such as *SST*, *OPRM1*, and *OPRK1*, with lower case-control cortical thickness scores being associated with higher gene expression. Reduced function of somatostatin-expressing inhibitory GABA neurons has also been implicated in a number of psychiatric conditions and MDD in particular (64,65), thus providing additional evidence for the overlap between MDD and stress circuitry.

Our findings of stress-induced enhanced connectivity between the striatum and amygdala with the insular, inferior frontal, and medial prefrontal areas and global cortical connectivity of frontoparietal areas fit theories postulating that acute stress increases alertness and activates the autonomic and central nervous systems to promote more adaptive behavior (2,8,18). Previous reviews also suggest an essential role for the salience (ventral attention) network in the acute stress response (8), and other studies have highlighted increased activation of the salience network in stressed

participants (66). Increased thalamocortical connectivity (67) during stress also supports our finding of increased striato-cortical connectivity because the thalamus is a key region in the cortico-basal-ganglia circuits (68). The lack of correlation between the FC changes and cortisol changes across groups suggests that the effects of acute stress on FC in the current study were at least partially distinct from the mediation of the stress response by cortisol. An analysis of the timescale of changes in FC and cortisol showed that throughout the experiment, the MAST first increased cortisol levels without affecting FC. Next, the MIST increased FC levels for several cortical and subcortical regions while cortisol levels both increased and decreased, with a small net increase in the overall group. Whereas our finding of increased hippocampal connectivity is consistent with previous studies that have shown that elevated corticosterone drives hippocampal activity within 10 to 60 minutes after stress exposure (13), other, non-cortisol-related mechanisms may be driving our hippocampal FC finding. Overall, our finding of FC changes in response to the MIST is more consistent with the activation of the monoaminergic system leading to shared recruitment and interplay in the cortico-subcortical circuits following stress (3).

Previous models suggested a balance between the salience and the frontoparietal control networks, whereby acute stress leads to a reallocation of resources to the salience network at the expense of the frontoparietal control network (69). However, we observed higher connectivity of both salience and frontoparietal networks to all other cortical regions. The hard MIST stress condition required participants to solve increasingly difficult, timed math problems while being given negative feedback about their performance. By contrast, the baseline condition required participants to solve simple math equations without time pressure. Therefore, the increased connectivity that emerged during the stress condition may be partially attributed to the increased cognitive demands and the stress caused by the presence of negative feedback.

While the imaging transcriptomics approach can leverage neuroimaging data to provide insights into molecular substrates of stress effects, our findings are limited in specificity and provide indirect, correlational rather than causal inferences (40,41). To obtain more direct evidence for the role of specific gene transcripts, participant-level gene expression data from deeply phenotyped samples are needed, although collecting such data can be costly and challenging. Recent advances in single-cell gene expression in postmortem brain samples of older adults (70,71) have generated valuable insights into the etiology of Alzheimer's disease, and future work on participant-level gene expression will similarly help advance our understanding of the mechanisms of psychiatric disorders. Together with many other genes with similar anatomical expression patterns including those involved in dopamine and glutamate signaling, we found *OPRM1*, *OPRK1*, *SST*, and *GABRA3/GABRA5* genes to be enriched in areas showing higher connectivity under stress. We focused on these genes given our hypotheses regarding GABAergic signaling, including in the somatostatin-expressing interneurons and the opioid system. We present some gene ontology analyses of the significant genes in the Supplement. However additional research is needed to test the extent to which these effects are unique to the opioid system.

We did not find significant group differences (e.g., clinical group, sex) in response to stress measured using a network-wide, whole-brain fMRI connectivity analytic approach (1). However, we had low statistical power to detect small to moderate effects using this approach, especially in the context of testing for 3-way interactions. In contrast, the use of a priori hypothesis-driven fMRI connectivity analyses of specific brain regions produced significant effects of interest modified by sex in the healthy control participants in the sample presented here (72). In fact, when a different acute negative stress reactivity task was used, some of these same stress circuitry regions were abnormal in MDD in adults (9) and were associated with hypothalamic-pituitary-adrenal axis dysregulation (73). Thus, future work on sex differences in gene expression associated with stress circuitry responses in MDD is needed, particularly given our previous work on sex differences in the genetic architecture of MDD (74). Finally, a substantial number of studies on stress in MDD have focused on severe stressors, especially in early life (5,75–79), thus demonstrating significant and robust dysfunction in MDD.

## Conclusions

In conclusion, we identified robust neural correlates of acute stress in a sample of participants who differed in MDD risk (healthy individuals and unmedicated individuals with past or current MDD). Gene expression analyses of a postmortem sample showed that stress altered FC in circuits that preferentially express *OPRM1*, *OPRK1*, *GABRA*, and *SST* genes, implicating genes that have also been strongly linked to imaging transcriptomics of depression (34,38). Finally, association analyses with PET maps of receptor density increased the specificity of our findings by showing that the stress effects on connectivity of striatal regions were not associated with high GABA<sub>A</sub> receptor density. Taken together, our findings highlight the role of the opioid system in stress and reward pathways that have previously been linked to depression.

## ACKNOWLEDGMENTS AND DISCLOSURES

This work was supported by the National Institute of Mental Health (NIMH) (Grant No. R01MH108602 [to multiple principal investigators, DAP and JMG]). In addition, DAP was partially supported by the NIMH (Grant Nos. P50 MH119467 and R37MH068376), and JMG and LMH was partially supported by the Office of Research on Women's Health-NIMH (Grant No. U54 MH118919). MI was supported by a Rappaport Mental Health Fellowship from McLean Hospital (Grant Nos. P20GM121312 and R01MH132565). PZ was supported by a Canadian Institutes of Health Research postdoctoral fellowship. The content is solely the responsibility of the authors and does not necessarily represent the official views of the National Institutes of Health.

We thank David Olson, M.D., Ph.D., for assistance with the blood collection protocol and Courtney Miller, R.N., for assistance with blood draws. We also thank Madeline (Lynn) Alexander, Ph.D., Laurie A. Scott, A.M., and Harlyn Aizley, Ed.M. for conducting clinical interviews to establish study eligibility and Monica Landi, M.S.W., for her help establishing diagnostic reliability. We used [BioRender.com](https://www.biorender.com) to create some of the Supplemental figures.

Presented in abstract form and as a poster at the 2023 Society of Biological Psychiatry annual meeting, April 27–April 29, 2023, San Diego, California.

Over the past 3 years, DAP has received consulting fees from Boehringer Ingelheim, Compass Pathways, Engrail Therapeutics, Neumora Therapeutics (formerly BlackThorn Therapeutics), Neurocrine Biosciences,

Neuroscience Software, Otsuka Therapeutics, Sage Therapeutics, Sama Therapeutics, and Takeda; he has received honoraria from the Psychonomic Society and American Psychological Association (for editorial work) and Alkermes; he has received research funding from the Brain and Behavior Research Foundation, Dana Foundation, Wellcome Leap, Millennium Pharmaceuticals, and the NIMH; he has received stock options from Compass Pathways, Engrail Therapeutics, Neumora Therapeutics, and Neuroscience Software. JMG is on the scientific advisory board and has an equity interest in Cala Health, a neuromodulation device company; this relationship is overseen by the Mass General Brigham Office for Industry Interactions and has no conflict with the work presented here. MM has served on the advisory board of Ipsen and AbbVie and served as a consultant for AbbVie and Sanofi. No funding or any involvement from these entities was used to support the current work, and all views expressed are solely those of the authors. All other authors report no biomedical financial interests or potential conflicts of interest.

## ARTICLE INFORMATION

From the Center for Depression, Anxiety and Stress Research, Department of Psychiatry, McLean Hospital, Harvard Medical School, Boston, Massachusetts (PZ, MI, JMD, ADM, KEN, MA, SME, DAP); Laureate Institute for Brain Research, The University of Tulsa, Tulsa, Oklahoma (MI); Department of Psychology, Yale University, New Haven, Connecticut (JMD); Department of Psychology and Neuroscience, University of Colorado Boulder, Boulder, Colorado (ADM); Department of Psychology, University of California, Los Angeles, Los Angeles, California (KEN); Gordon Center for Medical Imaging, Department of Radiology, Massachusetts General Hospital, Harvard Medical School, Boston, Massachusetts (MD, MN, NJG, GEF); Division of Women's Health, Brigham and Women's Hospital, Boston, Massachusetts (LMH, JMG); Innovation Center on Sex Differences in Medicine, Massachusetts General Hospital, Massachusetts General Hospital Research Institute, Harvard Medical School, Boston, Massachusetts (LMH, JMG); Clinical Neuroscience Laboratory of Sex Differences in the Brain, Department of Psychiatry, Massachusetts General Hospital, Harvard Medical School, Boston, Massachusetts (LMH, JMG); Division of Pediatric Endocrinology, Massachusetts General Hospital, Harvard Medical School, Boston, Massachusetts (MM); Department of Radiology, University of Pittsburgh, Pittsburgh, Pennsylvania (RN); Yale Positron Emission Tomography Center, Yale School of Medicine, New Haven, Connecticut (JMH, EDM); Department of Radiology and Biomedical Imaging, Department of Psychiatry, Yale School of Medicine, New Haven, Connecticut (JMH, EDM); and Departments of Psychiatry and Medicine, Harvard Medical School, Boston, Massachusetts (JMG).

PZ and MI contributed equally to this work as joint first authors.

Address correspondence to Diego A. Pizzagalli, Ph.D., at [dap@mclean.harvard.edu](mailto:dap@mclean.harvard.edu).

Received Sep 5, 2023; revised Jan 22, 2024; accepted Feb 10, 2024.

Supplementary material cited in this article is available online at <https://doi.org/10.1016/j.biopsych.2024.02.005>.

## REFERENCES

- van Oort J, Tendolkar I, Hermans EJ, Mulders PC, Beckmann CF, Schene AH, *et al.* (2017): How the brain connects in response to acute stress: A review at the human brain systems level. *Neurosci Biobehav Rev* 83:281–297.
- Yaribeygi H, Panahi Y, Sahraei H, Johnston TP, Sahebkar A (2017): The impact of stress on body function: A review. *Excli J* 16:1057–1072.
- Joëls M, Baram TZ (2009): The neuro-symphony of stress. *Nat Rev Neurosci* 10:459–466.
- Schneiderman N, Ironson G, Siegel SD (2005): Stress and health: Psychological, behavioral, and biological determinants. *Annu Rev Clin Psychol* 1:607–628.
- Pizzagalli DA (2014): Depression, stress, and anhedonia: Toward a synthesis and integrated model. *Annu Rev Clin Psychol* 10:393–423.
- Goldstein JM (2019): Impact of prenatal stress on offspring psychopathology and comorbidity with general medicine later in life. *Biol Psychiatry* 85:94–96.
- Kendler KS, Karkowski LM, Prescott CA (1999): Causal relationship between stressful life events and the onset of major depression. *Am J Psychiatry* 156:837–841.
- Valentino RJ, Van Bockstaele E (2015): Endogenous opioids: The downside of opposing stress. *Neurobiol Stress* 1:23–32.
- Holsen LM, Lancaster K, Klianski A, Whitfield-Gabrieli S, Cherkertzian S, Buka S, Goldstein JM (2013): HPA-axis hormone modulation of stress response circuitry activity in women with remitted major depression. *Neuroscience* 250:733–742.
- Dunn AJ, Swiergiel AH (2008): The role of corticotropin-releasing factor and noradrenaline in stress-related responses, and the inter-relationships between the two systems. *Eur J Pharmacol* 583:186–193.
- Koelsch S, Boehlig A, Hohenadel M, Nitsche I, Bauer K, Sack U (2016): The impact of acute stress on hormones and cytokines, and how their recovery is affected by music-evoked positive mood. *Sci Rep* 6: 23008.
- Droste SK, De Groot L, Atkinson HC, Lightman SL, Reul JMHM, Linthorst ACE (2008): Corticosterone levels in the brain show a distinct ultradian rhythm but a delayed response to forced swim stress. *Endocrinology* 149:3244–3253.
- Karst H, Berger S, Turiault M, Tronche F, Schütz G, Joëls M (2005): Mineralocorticoid receptors are indispensable for nongenomic modulation of hippocampal glutamate transmission by corticosterone. *Proc Natl Acad Sci USA* 102:19204–19207.
- Drolet G, Dumont EC, Gosselin I, Kinkead R, Laforest S, Trotter JF (2001): Role of endogenous opioid system in the regulation of the stress response. *Prog Neuropsychopharmacol Biol Psychiatry* 25:729–741.
- Valentino RJ, Volkow ND (2018): Untangling the complexity of opioid receptor function. *Neuropsychopharmacology* 43:2514–2520.
- Admon R, Holsen LM, Aizley H, Remington A, Whitfield-Gabrieli S, Goldstein JM, Pizzagalli DA (2015): Striatal hypersensitivity during stress in remitted individuals with recurrent depression. *Biol Psychiatry* 78:67–76.
- Vogel S, Klumpers F, Schröder TN, Oplaat KT, Krugers HJ, Oitzl MS, *et al.* (2017): Stress induces a shift towards striatum-dependent stimulus-response learning via the mineralocorticoid receptor. *Neuropsychopharmacology* 42:1262–1271.
- Goldstein JM, Holsen L, Cherkertzian S, Misra M, Handra RJ (2017): Neuroendocrine mechanisms of depression: Clinical and preclinical evidence. In: Charney DS, Nestler EJ, Sklar P, Buxbaum JD, editors. *Charney & Nestler's Neurobiology of Mental Illness*, 5 edition. New York: Oxford University Press.
- Jankord R, Herman JP (2008): Limbic regulation of hypothalamo-pituitary-adrenocortical function during acute and chronic stress. *Ann N Y Acad Sci* 1148:64–73.
- Nakagawasa O, Tadano T, Tan No K, Nijijima F, Sakurada S, Endo Y, Kisara K (1999): Changes in beta-endorphin and stress-induced analgesia in mice after exposure to forced walking stress. *Methods Find Exp Clin Pharmacol* 21:471–476.
- Lewis JW, Sherman JE, Liebeskind JC (1981): Opioid and non-opioid stress analgesia: Assessment of tolerance and cross-tolerance with morphine. *J Neurosci* 1:358–363.
- Contet C, Gavériaux-Ruff C, Matifas A, Caradec C, Champy MF, Kieffer BL (2006): Dissociation of analgesic and hormonal responses to forced swim stress using opioid receptor knockout mice. *Neuropsychopharmacology* 31:1733–1744.
- Ferdousi M, Finn DP (2018): Stress-induced modulation of pain: Role of the endogenous opioid system. *Prog Brain Res* 239:121–177.
- Miller GM, Bendor J, Tiefenbacher S, Yang H, Novak MA, Madras BK (2004): A mu-opioid receptor single nucleotide polymorphism in rhesus monkey: Association with stress response and aggression. *Mol Psychiatry* 9:99–108.
- Kennedy SE, Koeppe RA, Young EA, Zubieta JK (2006): Dysregulation of endogenous opioid emotion regulation circuitry in major depression in women. *Arch Gen Psychiatry* 63:1199–1208.
- Muschamp JW, Van't Veer A, Carlezon WA (2011): Tracking down the molecular substrates of stress: New roles for p38 $\alpha$  MAPK and kappa-opioid receptors. *Neuron* 71:383–385.

## Stress-Related Connectivity in Opioid-Rich Regions

27. Jacobson ML, Browne CA, Lucki I (2020): Kappa opioid receptor antagonists as potential therapeutics for stress-related disorders. *Annu Rev Pharmacol Toxicol* 60:615–636.
28. Krystal AD, Pizzagalli DA, Smoski M, Mathew SJ, Nurnberger JJ, Lisanby SH, *et al.* (2020): A randomized proof-of-mechanism trial applying the ‘fast-fail’ approach to evaluating  $\kappa$ -opioid antagonism as a treatment for anhedonia. *Nat Med* 26:760–768.
29. Pizzagalli DA, Smoski M, Ang YS, Whittton AE, Sanacora G, Mathew SJ, *et al.* (2020): Selective kappa-opioid antagonism ameliorates anhedonic behavior: Evidence from the Fast-fail Trial in Mood and Anxiety Spectrum Disorders (FAST-MAS). *Neuropsychopharmacology* 45:1656–1663.
30. Jelen LA, Stone JM, Young AH, Mehta MA (2022): The opioid system in depression. *Neurosci Biobehav Rev* 140:104800.
31. Gavioli EC, Holanda VAD, Ruzza C (2019): NOP ligands for the treatment of anxiety and mood disorders. *Handb Exp Pharmacol* 254:233–257.
32. Gavioli EC, Holanda VAD, Calo G, Ruzza C (2021): Nociceptin/orphanin FQ receptor system blockade as an innovative strategy for increasing resilience to stress. *Peptides* 141:17054.
33. Morgan SE, Seidlitz J, Whitaker KJ, Romero-García R, Clifton NE, Scarpazza C, *et al.* (2019): Cortical patterning of abnormal morphometric similarity in psychosis is associated with brain expression of schizophrenia-related genes. *Proc Natl Acad Sci USA* 116:9604–9609.
34. Anderson KM, Collins MA, Kong R, Fang K, Li J, He T, *et al.* (2020): Convergent molecular, cellular, and cortical neuroimaging signatures of major depressive disorder. *Proc Natl Acad Sci USA* 117:25138–25149.
35. Amatkevičiūtė A, Fulcher BD, Fornito A (2019): A practical guide to linking brain-wide gene expression and neuroimaging data. *Neuroimage* 189:353–367.
36. Amatkevičiūtė A, Markello RD, Fulcher BD, Misić B, Fornito A (2023): Toward best practices for imaging transcriptomics of the human brain. *Biol Psychiatry* 93:391–404.
37. Amatkevičiūtė A, Fulcher BD, Bellgrove MA, Fornito A (2021): Where the genome meets the connectome: Understanding how genes shape human brain connectivity. *Neuroimage* 244:118570.
38. Li J, Seidlitz J, Suckling J, Fan F, Ji GJ, Meng Y, *et al.* (2021): Cortical structural differences in major depressive disorder correlate with cell type-specific transcriptional signatures. *Nat Commun* 12:1647.
39. Writing Committee for the Attention-Deficit/Hyperactivity Disorder, Autism Spectrum Disorder, Bipolar Disorder, Major Depressive Disorder, Obsessive-Compulsive Disorder, and Schizophrenia ENIGMA Working Groups, *et al.* (2021): Virtual histology of cortical thickness and shared neurobiology in 6 psychiatric disorders. *JAMA Psychiatry* 78:47–63.
40. Mandal AS, Gandal M, Seidlitz J, Alexander-Bloch A (2022): A critical appraisal of imaging transcriptomics. *Biol Psychiatry Glob Open Sci* 2:311–313.
41. Amatkevičiūtė A, Fulcher BD, Bellgrove MA, Fornito A (2022): Imaging transcriptomics of brain disorders. *Biol Psychiatry Glob Open Sci* 2:319–331.
42. Markello RD, Amatkevičiūtė A, Poline JB, Fulcher BD, Fornito A, Misić B (2021): Standardizing workflows in imaging transcriptomics with the Abagen toolbox. *eLife* 10:1–27.
43. Dedovic K, Renwick R, Mahani NK, Engert V, Lupien SJ, Pruessner JC (2005): The Montreal Imaging Stress Task: Using functional imaging to investigate the effects of perceiving and processing psychosocial stress in the human brain. *J Psychiatry Neurosci* 30:319–325.
44. Ironside M, Moser AD, Holsen LM, Zuo CS, Du F, Perlo S, *et al.* (2021): Reductions in rostral anterior cingulate GABA are associated with stress circuitry in females with major depression: A multimodal imaging investigation. *Neuropsychopharmacology* 46:2188–2196.
45. Satterthwaite TD, Elliott MA, Gerraty RT, Ruparel K, Loughhead J, Calkins ME, *et al.* (2013): An improved framework for confound regression and filtering for control of motion artifact in the pre-processing of resting-state functional connectivity data. *Neuroimage* 64:240–256.
46. Glasser MF, Coalson TS, Robinson EC, Hacker CD, Harwell J, Yacoub E, *et al.* (2016): A multi-modal parcellation of human cerebral cortex. *Nature* 536:171–178.
47. Hansen JY, Shafiei G, Markello RD, Smart K, Cox SML, Nørgaard M, *et al.* (2022): Mapping neurotransmitter systems to the structural and functional organization of the human neocortex. *Nat Neurosci* 25:1569–1581.
48. urtonen O, Saarinen A, Nummenmaa L, Tuominen L, Tikka M, Armio RL, *et al.* (2021): Adult attachment system links with brain Mu opioid receptor availability in vivo. *Biol Psychiatry Cogn Neurosci Neuroimaging* 6:360–369.
49. Kantonen T, Karjalainen T, Isojärvi J, Nuutila P, Tuisku J, Rinne J, *et al.* (2020): Interindividual variability and lateralization of  $\mu$ -opioid receptors in the human brain. *Neuroimage* 217:116922.
50. Dukart J, Holiga Š, Chatham C, Hawkins P, Forsyth A, Mcmillan R, *et al.* (2018): Cerebral blood flow predicts differential neurotransmitter activity. *Sci Rep* 8:4074.
51. Vijay A, Cavallo D, Goldberg A, de Laat B, Nabulsi N, Huang Y, *et al.* (2018): PET imaging reveals lower kappa opioid receptor availability in alcoholics but no effect of age. *Neuropsychopharmacology* 43:2539–2547.
52. Tollefson S, Stoughton C, Himes ML, McKinney KE, Mason S, Ciccocioppo R, Narendran R (2023): Imaging nociceptin opioid peptide receptors in alcohol use disorder with [11C]NOP-1A and positron emission tomography: Findings from a second cohort. *Biol Psychiatry* 94:416–423.
53. Pruessner JC, Kirschbaum C, Meinischmid G, Hellhammer DH (2003): Two formulas for computation of the area under the curve represent measures of total hormone concentration versus time-dependent change. *Psychoneuroendocrinology* 28:916–931.
54. Smeets T, Cornelisse S, Quaedflieg CWEM, Meyer T, Jelčić M, Merckelbach H (2012): Introducing the Maastricht Acute Stress Test (MAST): A quick and non-invasive approach to elicit robust autonomic and glucocorticoid stress responses. *Psychoneuroendocrinology* 37:1998–2008.
55. Benjamini Y, Hochberg Y (1995): Controlling the false discovery rate: A practical and powerful approach to multiple testing. *J R Stat Soc B* 57:289–300.
56. Yeo BT, Krienen FM, Sepulcre J, Sabuncu MR, Lashkari D, Hollinshead M, *et al.* (2011): The organization of the human cerebral cortex estimated by intrinsic functional connectivity. *J Neurophysiol* 106:1125–1165.
57. Zhukovsky P, Wainberg M, Milic M, Tripathy SJ, Mulsant BH, Felsky D, Voineskos AN (2022): Multiscale neural signatures of major depressive, anxiety, and stress-related disorders. *Proc Natl Acad Sci USA* 119:e2204433119.
58. Zhukovsky P, Savulich G, Morgan S, Dalley JW, Williams GB, Ersche KD (2022): Morphometric similarity deviations in stimulant use disorder point towards abnormal brain ageing. *Brain Commun* 4:fcac079.
59. French L, Ma T, Oh H, Tseng GC, Sibille E (2017): Age-related gene expression in the frontal cortex suggests synaptic function changes in specific inhibitory neuron subtypes. *Front Aging Neurosci* 9:162.
60. Howard DM, Adams MJ, Shirali M, Clarke TK, Marioni RE, Davies G, *et al.* (2018): Genome-wide association study of depression phenotypes in UK Biobank identifies variants in excitatory synaptic pathways. *Nat Commun* 9:1470.
61. Howard DM, Adams MJ, Clarke TK, Hafferty JD, Gibson J, Shirali M, *et al.* (2019): Genome-wide meta-analysis of depression identifies 102 independent variants and highlights the importance of the prefrontal brain regions. *Nat Neurosci* 22:343–352.
62. Vijay A, Wang S, Worhunsky P, Zheng MQ, Nabulsi N, Ropchan J, *et al.* (2016): PET imaging reveals sex differences in kappa opioid receptor availability in humans, in vivo. *Am J Nucl Med Mol Imaging* 6:205–214.
63. Peciña M, Karp JF, Mathew S, Todtenkopf MS, Ehrich EW, Zubieta JK (2019): Endogenous opioid system dysregulation in depression: Implications for new therapeutic approaches. *Mol Psychiatry* 24:576–587.
64. Fee C, Banasr M, Sibille E (2017): Somatostatin-positive gamma-aminobutyric acid interneuron deficits in depression: Cortical microcircuit and therapeutic perspectives. *Biol Psychiatry* 82:549–559.

65. Sibille E (2017): Reduced somatostatin expression or somatostatin-positive gamma-aminobutyric acid neurons: A shared pathology across brain disorders. *Biol Psychiatry* 81:467–469.
66. Soares JM, Sampaio A, Ferreira LM, Santos NC, Marques P, Marques F, *et al.* (2013): Stress impact on resting state brain networks. *PLoS One* 8:e66500.
67. Maron-Katz A, Vaisvaser S, Lin T, Hendler T, Shamir R (2016): A large-scale perspective on stress-induced alterations in resting-state networks. *Sci Rep* 6:21503.
68. Haber SN (2016): Corticostriatal circuitry. *Dialogues Clin Neurosci* 18:7–21.
69. Hermans EJ, Henckens MJAG, Joëls M, Fernández G (2014): Dynamic adaptation of large-scale brain networks in response to acute stressors. *Trends Neurosci* 37:304–314.
70. Mathys H, Peng Z, Boix CA, Victor MB, Leary N, Babu S, *et al.* (2023): Single-cell atlas reveals correlates of high cognitive function, dementia, and resilience to Alzheimer's disease pathology. *Cell* 186:4365–4385.e27.
71. Sun N, Victor MB, Park YP, Xiong X, Scannail AN, Leary N, *et al.* (2023): Human microglial state dynamics in Alzheimer's disease progression. *Cell* 186:4386–4403.e29.
72. Cohen JE, Holsen LM, Ironside M, Moser AD, Duda JM, Null KE, *et al.* (2023): Neural response to stress differs by sex in Young adulthood. *Psychiatry Res Neuroimaging* 332:111646.
73. Mareckova K, Holsen L, Admon R, Whitfield-Gabrieli S, Seidman LJ, Buka SL, *et al.* (2017): Neural – Hormonal responses to negative affective stimuli: Impact of dysphoric mood and sex. *J Affect Disord* 222:88–97.
74. Blokland GAM, Grove J, Chen CY, Cotsapas C, Tobet S, Handa R, *et al.* (2022): Sex-dependent shared and nonshared genetic architecture across mood and psychotic disorders. *Biol Psychiatry* 91: 102–117.
75. Hammen C, Kim EY, Eberhart NK, Brennan PA (2009): Chronic and acute stress and the prediction of major depression in women. *Depress Anxiety* 26:718–723.
76. Hammen C (2005): Stress and depression. *Annu Rev Clin Psychol* 1:293–319.
77. Teicher MH, Andersen SL, Polcari A, Anderson CM, Navalta CP, Kim DM (2003): The neurobiological consequences of early stress and childhood maltreatment. *Neurosci Biobehav Rev* 27:33–44.
78. Teicher MH, Tomoda A, Andersen SL (2006): Neurobiological consequences of early stress and childhood maltreatment: Are results from human and animal studies comparable? *Ann N Y Acad Sci* 1071: 313–323.
79. Goldstein JM, Cohen JE, Mareckova K, Holsen L, Whitfield-Gabrieli S, Gilman SE, *et al.* (2021): Impact of prenatal maternal cytokine exposure on sex differences in brain circuitry regulating stress in offspring 45 years later. *Proc Natl Acad Sci USA* 118:1–8.

## SUPPLEMENTARY INFORMATION

### **Acute Stress Increases Striatal Connectivity With Cortical Regions Enriched for $\mu$ - and $\kappa$ -Opioid Receptors**

Zhukovsky *et al.*

## Supplementary Information

### Participants

All participants were unmedicated, right-handed, ages 18-25, had normal or corrected to normal vision, and were fluent in written and spoken English, able to provide informed consent, and were recruited from the greater Boston area. MDD participants met for DSM-5 criteria for MDD (as ascertained via Structured Clinical Interview for the DSM-5, SCID, performed by a PhD or MA-level clinician), had a baseline score >14 on the Beck Depression Inventory- II (BDI-II), and either a baseline score >16 on the Hamilton Depression Rating Scale (17-item, HAM-D) or a score of >12 on the, clinician administered, Quick Inventory of Depressive Symptomatology (QIDS-C). Remitted MDD (rMDD) participants met for at least one prior major depressive episode (MDE) lasting 2 months or longer or at least 2 MDEs lasting 2 weeks or longer in the past 5 years, depressed mood and anhedonia symptoms rating a 1 on the SCID with no more than two symptoms of depression reported at a mild degree (SCID rating of 2) eight weeks prior to testing, baseline BDI-II score  $\leq 9$ , and either baseline HAM-D score  $\leq 7$  or QIDS-C score  $\leq 5$ . Healthy controls (HCs) reported an absence of medical, neurological, and psychiatric illness (including alcohol and substance abuse), as assessed by the SCID, baseline BDI-II score  $\leq 9$ , and either baseline HAM-D score  $\leq 7$  or QIDS-C score  $\leq 5$ . Female participants were scanned during the follicular phase of their menstrual cycle. Recruitment strategy included stratifying by sex and ensuring HCs were comparable within sex by group.

Exclusion criteria included: MRI contraindications (i.e., non-approved metal, claustrophobia, injury or movement disorder that makes it difficult to lie still); women who were pregnant or currently breastfeeding; current use of hormone replacement therapy and/or anabolic steroids; diabetes with poor glucose control or diabetes controlled with Metformin; serious or unstable medical illness (i.e., cardiovascular, hepatic, renal, respiratory, endocrine, neurological, or hematologic disease); history of seizure or seizure disorder; history of significant head injury of concussion with loss of consciousness of two minutes or more, or head injury with lingering functional/psychological impact; history of chronic migraine (>15 days in a month); hypothyroidism, hyperthyroidism, or other thyroid disorder that is not controlled by medication; sickle cell anemia, Raynaud's disease, ulcerative skin diseases, hemophilia, current infectious illness (either transient or chronic, i.e., Lyme disease) at the MRI visit; illness currently receiving acute treatment (e.g., taking antibiotics) at the MRI visit; current episode of allergic reaction or asthma; history or current diagnosis of dementia; and evidence of significant inconsistencies in self-report.

Drug and/or substance use exclusion criteria included: use of greater than 10 cigarettes per day; history of greater than five uses of cocaine or illicit stimulants; greater than 10 lifetime uses of psilocybin mushrooms; history of greater than a cumulative five uses of ecstasy, LSD, MDMA or opioids (prescribed opioids for a limited period, i.e., post-surgery, was allowed if use was not in the past 3 months); history of regular marijuana use (5-7x/week) before the age of 15; greater than one lifetime use of inhalants, IV drugs, crack cocaine, or crystal methamphetamine; greater than five alcohol induced blackouts in lifetime; current use of psychotropic drugs; no use of dopamine affecting drug in the past two months (if participant(s) had used drug affecting dopamine >5x in lifetime) or past three weeks (if participant(s) had used drug affecting dopamine <5x in life), dopamine affecting drugs included: amphetamine salts (Ritalin), methylphenidate (Adderall), and apomorphine (Uprima); use of antibiotics 24hrs prior to scan, and/or use of melatonin five days prior to scan; and recent use (with 3 weeks scan) of any

medication that affected blood flow or blood pressure, or which is vasodilating/vasoconstricting. Additional drug/substance use exclusion criteria for MDDs and rMDDs only, included use of psychotropic medication for at least: six weeks for fluoxetine; six months for neuroleptics, two weeks for benzodiazepines and any other antidepressants.

Psychiatric exclusion criteria included history or current diagnosis of any of the following DSM-5 psychiatric illnesses: organic mental disorder, learning disabilities, autism or any other pervasive developmental disorder, schizophrenia, schizoaffective disorder, delusional disorder, psychotic disorders not otherwise specified, bipolar disorder, OCD, anorexia nervosa, somatoform disorders, severe borderline or antisocial personality disorder, mild alcohol or non-marijuana substance use disorder within the last 12 months (cocaine or stimulant abuse at any time will lead to exclusion); specific phobia, social anxiety disorder, and generalized anxiety disorder or cannabis use disorder were allowed only if secondary to MDD; a history of PTSD, bulimia, binge eating disorder, or panic disorder were allowed only if secondary to MDD and in remission for >2 years; a history of ADHD was allowed on a case-by-case basis only if secondary to MDD. Further exclusion criteria included displays of mood congruent or mood incongruent psychotic features; suicidal ideation where outpatient treatment was determined to be unsafe by study clinicians (referral to appropriate treatment was provided); lifetime history of electroconvulsive therapy (ECT); and having a first-degree relative (parents or sibling) with a history of a psychotic disorder or psychotic symptoms. For rMDD participants only: no diagnosis of anxiety disorders in the past two months, other than social anxiety disorder.

### **MRI acquisition details**

A magnetization-prepared rapid acquisition (MPRAGE) sequence was used to acquire T1 structural data. The T1 image acquisition parameters were as follows: repetition time (TR) = 2530 ms; echo times (TE) = 1.69, 3.55, 5.41 and 7.27 ms; field of view = 256 mm; voxel dimensions = 1.0 x 1.0 x 1.0 mm<sup>3</sup>; 176 slices. A gradient echo T2\*-weighted echo planar imaging (EPI) sequence was used to acquire functional MRI data. The fMRI sequence acquisition parameters were as follows: repetition time (TR) = 2000 ms; echo time (TE) = 30 ms; field of view = 204 mm; voxel dimension = 1.5 x 1.5 x 1.5 mm; 84 interleaved slices with a multiband acceleration factor of 3.

### **MRI QC exclusions**

Among the 129 participants with imaging data, one was not included due to failed MRI quality control, one due to excessive dropout, another participant restarted the experiment, and two participants had excessive motion, resulting in 125 participants with usable fMRI data on at least one run. Among these participants, ten individuals had excessive motion during baseline or the stress condition. Motion was assessed as follows [1]: frames that exceeded a threshold of 0.5 mm FD or 1.5 standardized DVARS were annotated as motion outliers. Any participant with >20% motion outliers per run was excluded from analysis.

### **MRI Processing**

As part of fMRIPrep processing, BOLD runs were slice-time corrected using 3dTshift from AFNI and resampled to the fsaverage and MNI152NLin6Asym spaces.

## Global and subcortical FC measures

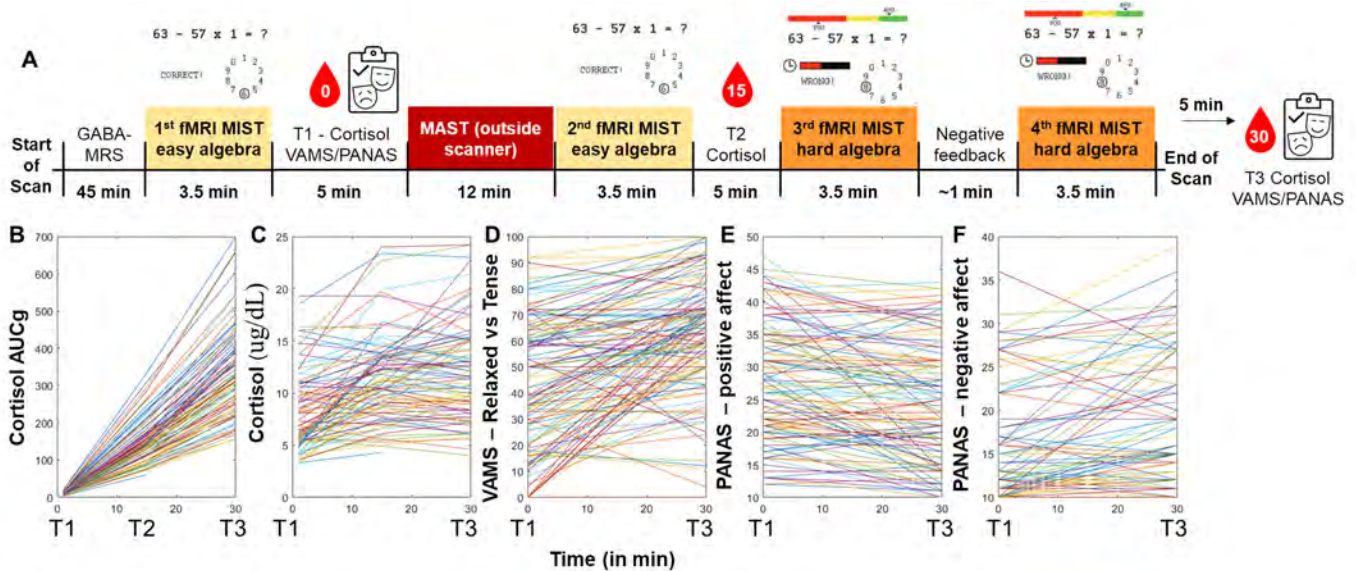
In calculating global cortical FC, we followed Cole et al [2,3]. We first calculated pairwise connectivity matrix between bilateral regions of interest from the HCP parcellation [4], resulting in a 180x180 r-to-z transformed correlation matrix using FSLNets (<https://fsl.fmrib.ox.ac.uk/fsl/fslwiki/FSLNets>). We used the direct Pearson's correlations, a very common approach to undirected functional connectivity. We then excluded the values along the diagonal given that the connectivity between a region and itself is always equal to one. We averaged each row of the resulting matrix to obtain the connectivity of each cortical region to all other cortical regions, which we refer to as global cortical connectivity. In calculating subcortical connectivity values, we also used FSLNets on the subcortical and cortical timeseries to estimate transformed Pearson's correlations between each subcortical region and cortical timeseries from the HCP parcellation.

## Stress induction details

The study protocol is described in more detail by Ironside et al [1] and Figure 1 in the main text, visualizes all tests and biomarkers collected as part of the study. Specifically, participants first completed an fMRI scan while solving easy algebra problems, which was the 'baseline' imaging condition. The scanner table was then pulled out and they completed the MAST (Maastricht Stress Test). This involved alternating trials of uncertain duration (determined by the computer) where participants are instructed to submerge their hand in ice-cold water and complete mental arithmetic under supervision from two unempathetic doctors. Immediately afterwards, the scanner table was retuned and they completed the second fMRI scan while also solving easy algebra problems in the scanner. Following a blood sample collection, they then completed the third fMRI scan in the 'hard MIST' condition, which required participants to solve complicated algebra problems under time pressure with visual feedback on the screen that they were performing below average. They then received negative feedback on their performance over the intercom from the control room of the MRI scanner and went on to complete the fourth fMRI scan, which was also a 'hard MIST' condition in which they solved complex algebra problems under time pressure and negative visual feedback. The last scan was followed by blood sample collection. Each fMRI scan lasted 3.5 minutes. In our analyses we aimed to specifically test the effects of stress on functional connectivity; consequently, we compared functional connectivity during the fourth fMRI run, i.e. the condition with the expected highest degree of cumulative stress, with functional connectivity at baseline. Cortisol level increases [1] confirmed stress induction. We provide an overview of the study procedures in Supplementary Figure 1.

We included both MAST and MIST stress induction paradigms for two reasons: firstly, we wanted to generate a cumulative amount of stress, by including several stress manipulations, starting with the MAST and introducing additional stressors using the MIST paradigm. Piloting also supported the addition to the MAST as a more potent stressor compared to the MIST. The MAST requires participants to submerge their hand in ice-cold water for a period of time unknown to them and occurs outside the scanner. Some participants may experience relief once they are allowed to take their hand out of the ice water. Second, it is a physical stressor and while it is potent for many participants, it may not affect all individuals to the same degree. We conducted an fMRI session (2<sup>nd</sup> run) with the 'easy' MIST and a blood draw immediately following the MAST to specifically assess the effects of the MAST. It also provided an additional control condition for assessing the effects of the blood draw and the scan itself. Following the MAST, we added an 'online' stressor ('hard' MIST) that occurred during the scan (3<sup>rd</sup> run). We

collected two runs of fMRI data during the ‘hard’ MIST that provided negative feedback to participants, telling them that they were performing well below average at solving complex mathematical problems. While in the main text we show specifically the comparison between the fourth run of fMRI and baseline, in the Supplemental Information we also provide the results from the comparison of the third run of fMRI vs baseline and the results from the comparison of the second run of fMRI vs baseline.



**Supplementary Figure 1.** Overview of the study design, adapted from Ironside et al [1]. A timeline of the assessments (A) shows that there were three blood draws. The first blood draw (T1) occurred immediately following the first fMRI scan and preceding the MAST intervention. The second blood draw (T2) occurred immediately following the second fMRI scan and preceding the ‘hard’ MIST. During the ‘hard’ MIST condition participants experienced stress induction during the scan. Finally, the third blood draw (T3) occurred following two rounds of the ‘hard’ MIST condition, once the participants exited the scanner. At T1 and T3, questionnaires assessing participants’ subjective experience of stress were collected using VAMS (Visual Analogue Mood Scale) and PANAS (Positive and Negative Affective Schedule[5]). We found a significant effect of time (and consequently of the accumulation of different stress manipulations) on cumulative cortisol levels (AUCg, B), absolute cortisol levels (C) the VAMS subscale assessing participants’ feeling relaxed vs tense (D), a significant decrease in positive (E) and a significant increase in negative (F) affect on the PANAS.

### Analysis of stress effects on cortisol and self-reported subjective experience of stress

A linear mixed effect model ( $Cortisol\ AUCg \sim sex + age + time + (1 + time | Participant)$ ) revealed a significant effect of time ( $\beta=160.7$ ,  $SE=6.275$ ,  $t(268)=25.61$ ,  $p<0.001$ ) on cumulative cortisol levels and on absolute cortisol levels ( $\beta=1.846$ ,  $SE=0.231$ ,  $t(268)=7.979$ ,  $p<0.001$ ). The stepwise increases in cortisol levels from baseline (T1) to post-MAST at T2 ( $p=3 \times 10^{-15}$ ), and from T2 to post-MIST at T3 ( $p=0.012$ ), are shown in Supplementary Figure 1B. Similarly, mixed effect models (*fitlme*, MATLAB R2022a) showed that, compared to baseline (T1), participants felt more tense (Figure 1C,  $\beta=19.945$ ,  $SE=2.057$ ,  $t(245)=9.697$ ,  $p<0.001$ ), felt less positive affect (Figure 1D,  $\beta=-3.089$ ,  $SE=0.583$ ,  $t(240)=5.296$ ,  $p<0.001$ ) and more negative affect (Figure 1E,  $\beta=2.412$ ,  $SE=0.415$ ,  $t(240)=5.825$ ,  $p<0.001$ ) following the MAST

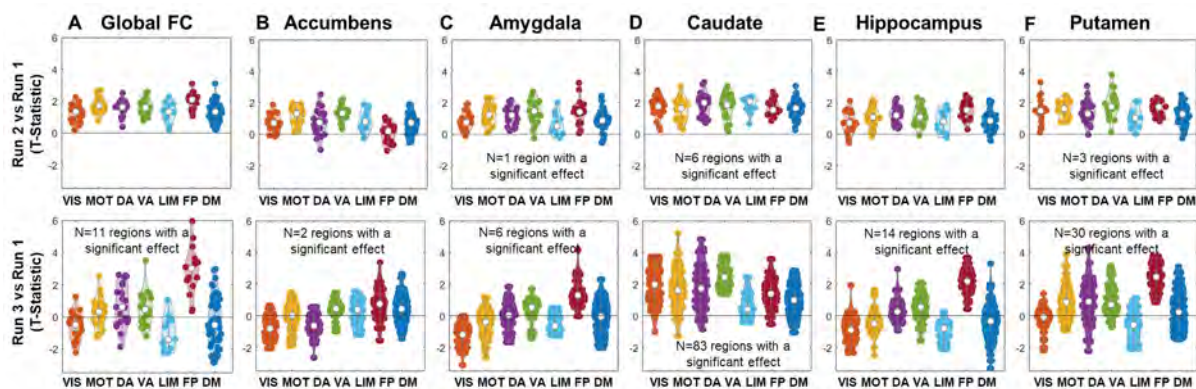
and MIST induction (T3). Cortisol levels increased throughout the scanning session, suggesting rising or sustained levels of stress throughout the scan. Among the 89 participants with cortisol data for T1 and T2, we found an increase in cortisol levels at T2 relative to T1 for 67 participants; a decrease among 20 participants and no change in cortisol level among 2 participants. Among the 86 participants with cortisol data for T2 and T3, we found an increase in cortisol levels at T3 relative to T2 for 47 participants and a decrease for 39 participants. The proportion of participants with increases vs decreases in cortisol was significantly different for T1 to T2 compared to T2 to T3 ( $X^2(1, N=173)=9.622, p=0.002$ ). Finally, at T3, cortisol levels returned to below-baseline levels for only 21 of 90 participants with cortisol data at T1 and T3.

### Analysis of stress effects on FC during the 2<sup>nd</sup> and 3<sup>rd</sup> fMRI runs compared to baseline

First, we repeated the analyses shown in Figure 1 of the main text, comparing the 2<sup>nd</sup> fMRI run that occurred immediately after the MAST test with the 1<sup>st</sup> baseline fMRI run. Highlighting the specificity of the findings shown in the main text, we found no significant differences in cortical or subcortical FC ( $p_{FDR}>0.05$ ) between this 2<sup>nd</sup> run of fMRI and baseline, during which participants solved easy algebraic problems. We show the distribution of the effects of fMRI run ('easy' MIST immediately following the MAST, i.e., run 2 vs 'easy' MIST preceding the MAST, i.e., run 1) on cortical and subcortical FC across the Yeo 7 networks in Supplementary Figure 2 (top row).

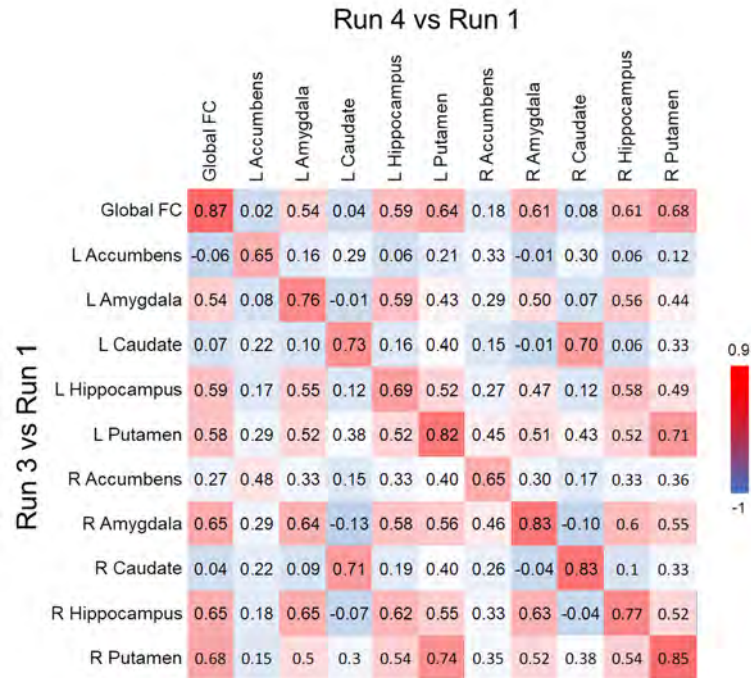
However, we found a large number of significant differences between the 3<sup>rd</sup> run of fMRI (i.e., 'hard' MIST with complex algebraic problems and negative feedback) vs baseline.

Supplementary Figure 2 (bottom row) summarizes the distribution of the effects of fMRI run ('hard' MIST, i.e., run 3 vs 'easy' MIST preceding the MAST, i.e., run 1) on cortical and subcortical FC across the Yeo 7 networks. This finding reinforces our central finding that acute stress during the 'hard' MIST is driving the effects we observed on functional connectivity.



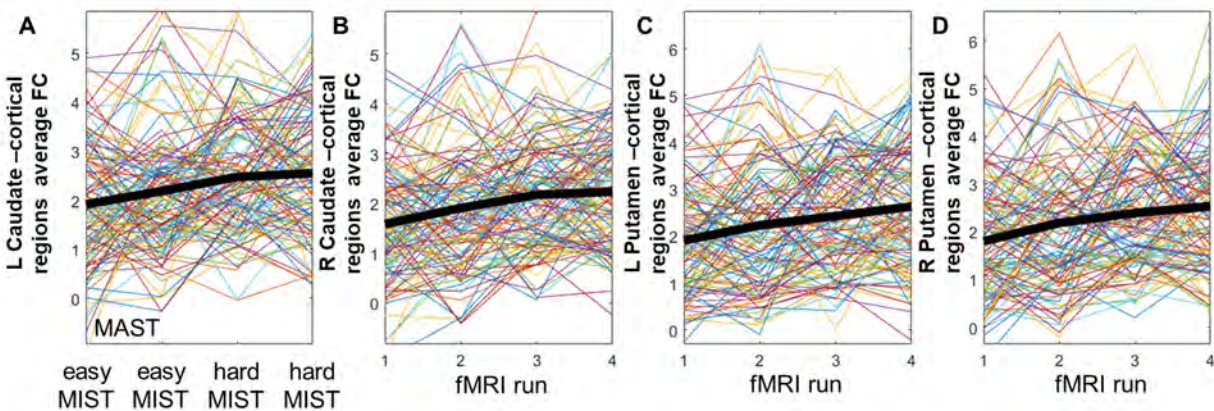
**Supplementary Figure 2.** Regional effects of the 'easy' MIST conducted immediately after the MAST stress induction (run 2) and regional effects of the first 'hard' MIST (run 3) on cortical (A) and subcortical (B-F) connectivity grouped by Yeo 7 networks are plotted in the top and bottom row, respectively.

We found that the pattern of differences between the 3<sup>rd</sup> run of fMRI vs baseline was very similar to the pattern of effects of the 4<sup>th</sup> run of fMRI (also 'hard' MIST with complex algebraic problems and negative feedback), as shown by the diagonal correlations in Supplementary Figure 3.



**Supplementary Figure 3.** Correlations between brain maps reflecting stress effects assessed in the first run of the ‘hard’ MIST (run 3) and in the second run of the ‘hard’ MIST (run 4) on cortical and subcortical connectivity. Correlations in the diagonal of the matrix show the similarity between brain maps of the same measure (e.g. effects of run 3 on Global FC vs effects of run 4 on Global FC).

Supplementary Figure 4 summarizes the change in FC of subcortical regions with the cortical regions identified as significant in the main analyses (Figure 1) over time (runs 1-4), highlighting the pronounced increases in FC in runs 3 and 4, i.e. hard MIST.



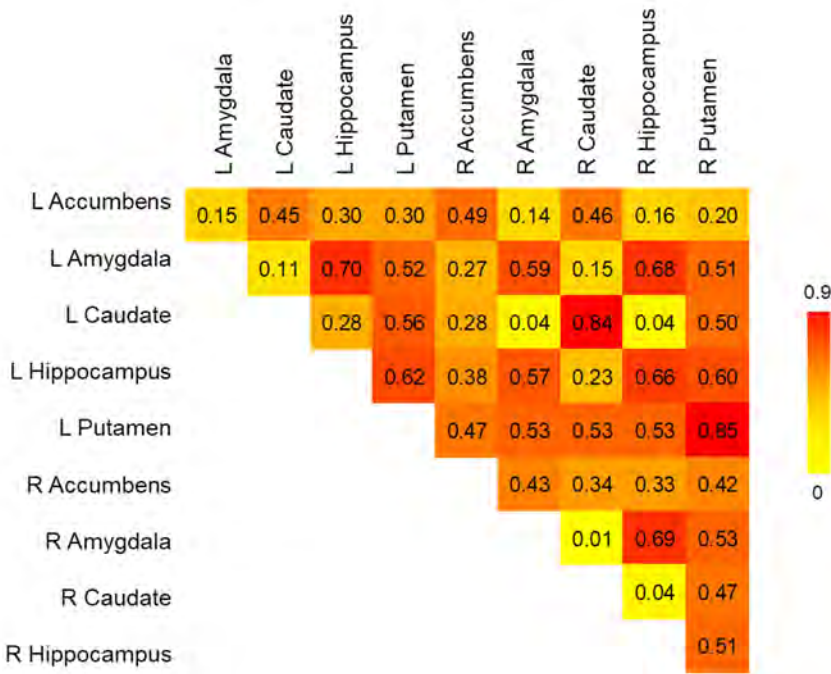
**Supplementary Figure 4.** Change in FC of the left (A) and right (B) caudate and left (C) and right (D) putamen with the cortical regions identified in the main analyses (Figure 1). Average FC across participants highlighted as a thick line shows that run 4 is characterized by the largest increases relative to baseline occurred during the ‘hard’ MIST, i.e., fMRI runs 3 and 4.

### Analysis of group x stress effects on FC

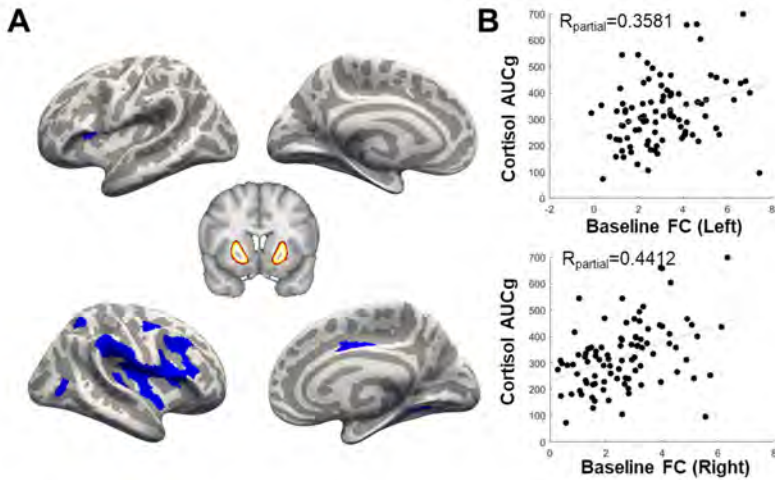
We focused on the hard MIST condition to test for the effects of stress. Between baseline and our 'hard MIST' condition, participants also experienced the MAST (Maastricht Stress Test) during which they submerge their hand in ice-cold water and completed mental arithmetic under supervision while they were outside the scanner. Therefore, the cortisol increase occurred over a period of time that covered these stressors. In addition to the main effects of stress (Model 1), we also tested for the group  $\times$  stress interactions as shown in Model 2:

*Model 2: FC ~ mean FD + sex + age + group \* stress + group + stress + (1 | Participant)*

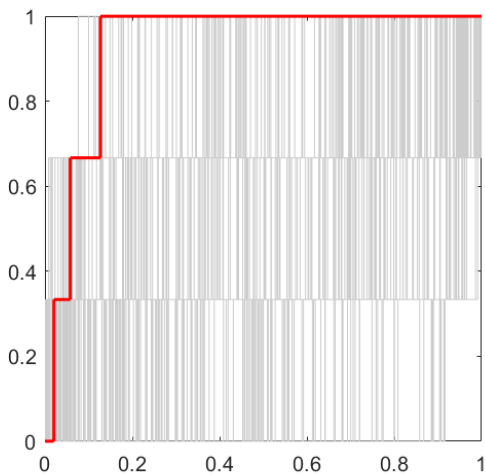
However, we did not find any significant interactive effects after FDR ( $q < 0.05$ ) correction [6].



**Supplementary Figure 5.** Correlations between brain maps reflecting stress effects on subcortical connectivity.



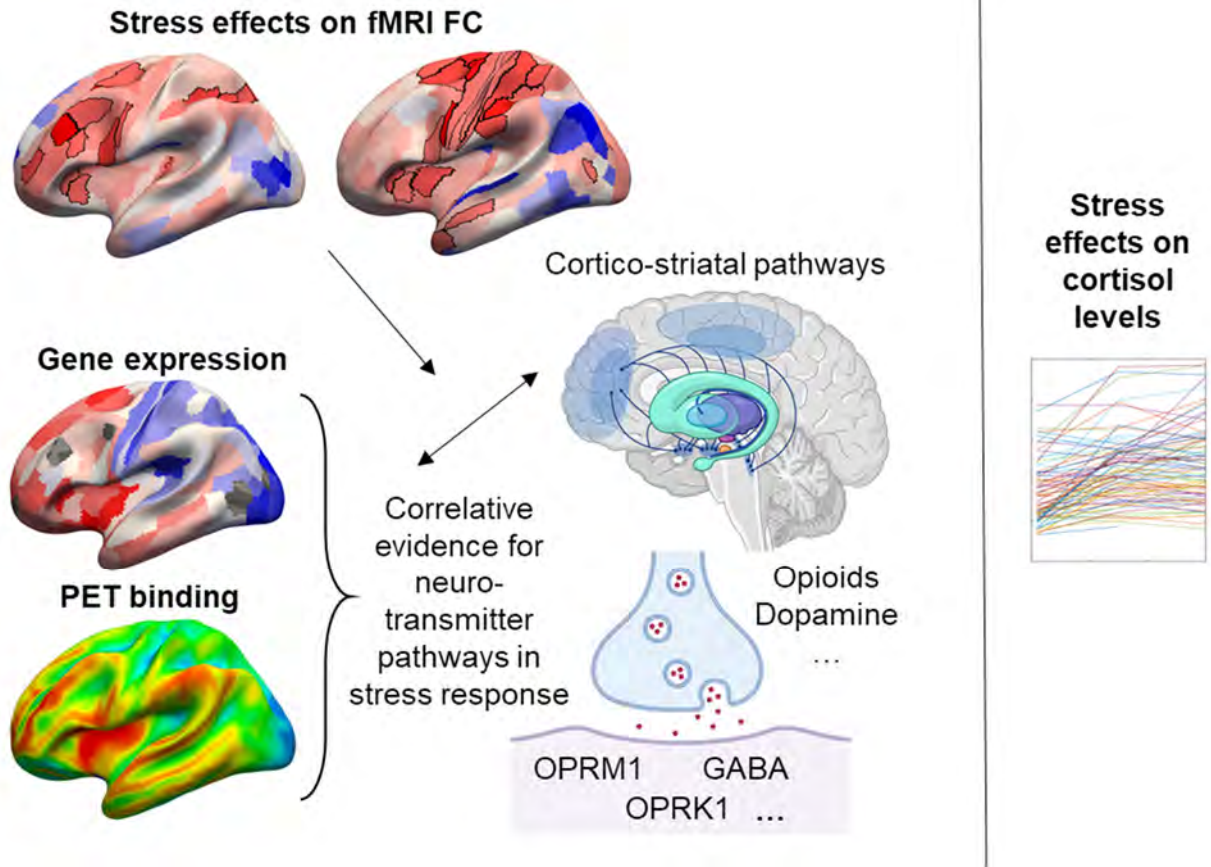
**Supplementary Figure 6.** Higher baseline functional connectivity of the putamen with cortical regions shown in blue (A) was associated with greater increase in cortisol levels under stress ( $p_{\text{FDR}} < 0.05$ ). Correlations between average putamen connectivity with the significant regions and cortisol increase are shown in (B); left putamen  $p = 5.7 \times 10^{-4}$ ; right putamen  $p = 1.5 \times 10^{-5}$ . Similar effects were observed with absolute levels of cortisol instead of the AUCg cumulative measure.



**Supplementary Figure 7.** AUC for somatostatin markers *SST*, *NPY*, *CORT* (in red) plotted against AUCs generated from random permutations ( $p = 0.028$ ).



**Supplementary Figure 8.** Gene ontology analysis of the PLS results.



**Supplementary Figure 9.** Conceptual overview of findings and approach. Stress effects on global cortical and subcortical-to-cortex connectivity has implicated cortico-striatal pathways in stress response. Imaging transcriptomic and PET analyses have further implicated opioid, GABA and monoamine signalling in acute stress response, among other neurochemical pathways. These findings were somewhat distinct from stress-related changes in cortisol levels, consistent with previously proposed temporal profiles of different stress mediators [7].

## References

1. Ironside M, Moser AD, Holsen LM, Zuo CS, Du F, Perlo S, et al. Reductions in rostral anterior cingulate GABA are associated with stress circuitry in females with major depression: a multimodal imaging investigation. *Neuropsychopharmacology*. 2021;46:2188–2196.
2. Cole MW, Yarkoni T, Repovš G, Anticevic A, Braver TS. Global connectivity of prefrontal cortex predicts cognitive control and intelligence. *J Neurosci*. 2012;32:8988–8999.
3. Cole MW, Anticevic A, Repovs G, Barch D. Variable Global Dysconnectivity and Individual Differences in Schizophrenia. *BPS*. 2011;70:43–50.
4. Glasser MF, Coalson TS, Robinson EC, Hacker CD, Harwell J, Yacoub E, et al. A multi-modal parcellation of human cerebral cortex. *Nature*. 2016;536:171–178.
5. D W, LA C, A T. Development and validation of brief measures of positive and negative affect: the PANAS scales. *J Pers Soc Psychol*. 1988;54:1063–1070.
6. Benjamini Y, Hochberg Y. Controlling the False Discovery Rate: A Practical and Powerful Approach to Multiple Testing. *J R Stat Soc Ser B*. 1995;57:289–300.
7. Joëls M, Baram TZ. The neuro-symphony of stress. *Nat Rev Neuro*. 2009;10:459–466.